



The dynamics of complex-amplitude norm-preserving lattices of coupled oscillators

Marcos V. Vessen Jr.^a, Paulo C. Rech^{a,b}, Marcus W. Beims^a,
José A. Freire^a, M.G.E. da Luz^a, Pedro G. Lind^{c,d,*},
Jason A.C. Gallas^{a,c,d}

^a*Departamento de Física, Universidade Federal do Paraná, Curitiba 81531-990, Brazil*

^b*Departamento de Física, Universidade do Estado de Santa Catarina, Joinville 89223-100, Brazil*

^c*Instituto de Física, Universidade Federal do Rio Grande do Sul, Porto Alegre 91501-970, Brazil*

^d*Institut für Computer Anwendungen, Universität Stuttgart, Pfaffenwaldring 27,
D-70569 Stuttgart, Germany*

Received 5 February 2004

Abstract

We introduce a class of models composed by lattices of coupled complex-amplitude oscillators which preserve the norm. These models are particularly well adapted to investigate phenomena described by the nonlinear Schrödinger equation. The coupling between oscillators is parameterized by the mass, while their local dynamics is illustrated for two area-preserving maps: one obtained from the exact local solution of the Schrödinger equation, the other obtained from its Crank–Nicholson discretization. In both cases, we determine all periodic orbits and show how to detect artifacts introduced by the discretization.

© 2004 Elsevier B.V. All rights reserved.

PACS: 05.45.Ra; 05.45.–a; 05.45.Mt

Keywords: Non-linear Schrödinger equation; Norm preservation; Coupled maps

1. Introduction

The interplay of nonlinearities in spatially continuous nonlinear systems is nowadays a subject of intensive research [1,2]. Paradigmatic systems consist of either lattices

* Corresponding author. Institut für Computer Anwendungen, Universität Stuttgart, Pfaffenwaldring 27, D-70569 Stuttgart, Germany.

E-mail address: lind@ica1.uni-stuttgart.de (P.G. Lind).

of nonlinear oscillators, governed locally by an ordinary differential equation (ODE) [3], or partial differential equations (PDEs). While lattices of coupled ODEs are most suitable for phenomena in the scale of interoscillator distances with a small number of oscillation modes, PDEs are more convenient for phenomena with large length scales or with a large number of oscillation modes.

One model studied in these two different contexts is the nonlinear Schrödinger equation [3,4], Eq. (1) below. The nonlinear Schrödinger PDE is used to model the formation of vortex lattices in a weakly interacting Bose condensed gas [5] and to model the evolution of monochromatic waves in pulse propagation along optical fibers [6], while its discretization in space yields the so-called discrete nonlinear Schrödinger equation [7], which can be used to study the processes underlying the localization of energy in nonlinear lattices [8,9], to study pairwise soliton collisions [10], to model three-dimensional Josephson–Junction arrays in the quantum regime [11] and discrete breathers in discrete nonlinear extended systems [7,12]. However, the continuous approximation of coupled ODEs into PDEs is frequently difficult to handle.

To overcome this difficulty it has been proposed [13] to discretize time as well, obtaining a lattice of coupled oscillators evolving with discrete time, the so-called coupled map lattices (CMLs). CMLs have been widely used to study reaction-diffusion systems [13], self-organized behavior spatial extended systems [14], diffusive transport in Hamiltonian systems [15], information capacity and pattern formation in networks [16], transport phenomena due to the competition between diffusion and advection [17], universality classes in spatial extended discrete systems [18], and also to model spiking–bursting neural behavior [19] and other synchronization phenomena [20].

In all these applications the local amplitudes of CMLs are assumed to be real and, in general, there is no need to impose physical constraints on them such as, e.g. norm preservation. However, for certain specific models in quantum physics, such as the nonlinear Schrödinger equation, one works with complex amplitudes which must preserve the norm during evolution. Moreover, although one-dimensional discrete maps have already been occasionally used in quantum chaos (as, for example, in Ref. [21]), as far as we know there is no complete formulation of spatially extended *quantum* systems evolving with *discrete*-time local dynamics.

In this paper, we introduce a CML model in which local amplitudes are complex and the norm is preserved all over the system. The CML model is introduced in Section 2, while in Section 3 two possible local dynamics are studied, namely the area-preserving exponential map and its Crank–Nicholson discretization. Discussion and conclusions are given in Section 4.

2. The norm-preserving CML model

The model we introduce below is well adapted to handle the nonlinear Schrödinger equation, namely

$$i \frac{\partial \Psi_x^t}{\partial t} = -\gamma \nabla^2 \Psi_x^t + (\lambda |\Psi_x^t|^2 + U(x)) \Psi_x^t, \quad (1)$$

where Ψ_x^t is the wave function, x and t label space and time, respectively, i is the imaginary unit, and $\gamma = \hbar^2/(2m)$, with m symbolizing the mass. Here $\lambda = g/\hbar$, g a real constant, represents the potential created by the boson density in the system, and $U(x) = (V(x) - \mu)/\hbar$, where $V(x)$ and μ represent the external and chemical potentials, respectively. As usual, we confine the system to a box of size L and assume periodic boundary conditions: $\Psi_0^t \equiv \Psi_L^t$.

Differently from the usual reaction–diffusion equations for chemical or hydrodynamical systems, here the norm is preserved: $\int |\Psi_x^{t+\Delta t}|^2 dx = \int |\Psi_x^t|^2 dx$. Nevertheless, Eq. (1) may be still regarded as a sort of reaction–diffusion equation, whose first term on the right is the diffusive ‘non-local’ contribution, while the second term represents the local evolution. The standard way of discretizing Eq. (1) is to consider a sort of splitting method [22] where local and non-local terms are discretized separately in two successive steps. The ‘local’ step corresponds to the exact solution of Eq. (1) when the diffusive (non-local) term is removed

$$\Psi_x^{t+\Delta t} = e^{-i\Delta t(\lambda|\Psi_x^t|^2 + U(x))} \Psi_x^t. \tag{2}$$

The ‘non-local’ step, solution of Eq. (1) when the ‘local’ term is removed, is obtained from the Crank–Nicholson discretization [22], given by the mean of the explicit and implicit schemes computed between t and $t + \Delta t$, namely

$$\begin{aligned} \frac{i}{2} [\Psi_x^{t+\Delta t} - \Psi_x^t] = & - \frac{\gamma \Delta t}{(\Delta x)^2} [\Psi_{x+\Delta x}^t + \Psi_{x-\Delta x}^t - 2\Psi_x^t + \Psi_{x+\Delta x}^{t+\Delta t} \\ & + \Psi_{x-\Delta x}^{t+\Delta t} - 2\Psi_x^{t+\Delta t}]. \end{aligned} \tag{3}$$

Although this expression is useful to study the nonlinear Schrödinger equation, it is not adequate for our purposes, since for CML models one must have each $\Psi_x^{t+\Delta t}$ as functions of Ψ_x^t alone, and from Eq. (3) one clearly sees this not to be the case. So, instead of the above usual procedure, we compute the explicit scheme between t and $t + \Delta t$ and the implicit scheme between $t - \Delta t$ and t , i.e., $\Psi_x^{\pm \Delta t} = [1 \pm i\gamma\Delta t\nabla^2]\Psi_x^t$. Thus, after performing the discretization of the diffusive operator, the ‘non-local’ step reads

$$\frac{i}{2} [\Psi_x^{t+\Delta t} - \Psi_x^{t-\Delta t}] = - \frac{\gamma \Delta t}{(\Delta x)^2} [\Psi_{x+\Delta x}^t + \Psi_{x-\Delta x}^t - 2\Psi_x^t] \tag{4}$$

which still preserves the norm, now between $t - \Delta t$ and $t + \Delta t$, and is unconditionally stable. Finally, substituting $t \rightarrow t + \Delta t$ with $\Delta t = \frac{1}{2}$ and $x \rightarrow j$, one arrives at the CML equivalent of the nonlinear Schrödinger equation, namely,

$$\Psi_j^{t+1} = \Psi_j^t + \gamma[F(\Psi_{j+1}^t) + F(\Psi_{j-1}^t) - 2F(\Psi_j^t)], \tag{5}$$

where $F(\Psi_j^t) = i\Psi_j^{t+1/2}$ with $\Psi_j^{t+1/2}$ defined either by Eq. (2) for $\Delta t = \frac{1}{2}$, or by another suitable discretization. Here $j = 1, \dots, L$ and periodic boundary conditions impose $\Psi_j \equiv \Psi_{j+L}$. Eq. (5) defines a CML with complex local amplitudes, whose coupling parameter γ is parameterized by the mass of each oscillator and where the norm is globally preserved, i.e., $\sum_{j=1}^L |\Psi_j^{t+1}|^2 = \sum_{j=1}^L |\Psi_j^t|^2$.

Similarly as for reaction–diffusion equations, where a CML is obtained when one interprets different contributions of the discretized operator as systems by themselves

[13], one could regard Eq. (5) as a system of coupled quantum systems ('oscillators'). Of course, this latter case requires imposing norm preservation for individual oscillators, in other words, the map $F(\Psi_j^t) = i\Psi_j^{t+1/2}$ must be area-preserving.

3. Area-preserving local dynamics

In the remainder, we study two area-preserving maps, the exponential map

$$\Psi_{t+1/2} = F_1(\Psi_t) = i e^{-i(a|\Psi_t|^2 + b_j)} \Psi_t, \quad (6)$$

obtained directly from Eq. (2) with $a = \lambda/2$ and $b_j = U_j/2$, and the map

$$\Psi_{t+1/2} = F_2(\Psi_t) = i \frac{1 - i(a|\Psi_t|^2 + b_j)}{1 + i(a|\Psi_t|^2 + b_j)} \Psi_t \quad (7)$$

which we call the Crank–Nicholson map since it is deduced from the Crank–Nicholson scheme of Eq. (2) with $a = \lambda/4$ and $b_j = U_j/4$. Both maps involve parameters which are suitable scalings of the potentials.

Now, we determine analytically all periodic orbits for the maps above and compare them. The differences between both maps are due to artifacts eventually introduced by the Crank–Nicholson scheme when discretizing the exact solution in Eq. (2). For simplicity, we set $b \equiv b_j$.

To determine all periodic orbits we separate real and imaginary parts on both sides of the map and change to polar coordinates, obtaining a two-dimensional area-preserving map of the form

$$r_{t+1} = r_t, \quad \theta_{t+1} = \theta_t + 2\pi\phi(r_t), \quad (8)$$

where, for $\Psi_t \equiv x_t + iy_t$, one has $r_t = \sqrt{x_t^2 + y_t^2}$ and $\theta_t = \arctan(y_t/x_t)$. While $r_{t+1} = r_t$ assures norm preservation, the other equation determines whether the orbit is periodic or not: for rational $\phi(r_t)$ one finds a periodic orbit on the circumference centered at the origin with radius r_t , while for irrational $\phi(r_t)$ the corresponding orbit fills densely the circumference, being quasi-periodic. Periodic orbits with period k are solutions of $\phi(r_t) = p/k$, with p an integer between 1 and $k - 1$ and k and p are relative primes.

For the exponential map in Eq. (6) one obtains $\phi(r_t) = (\pi/2 - ar_t^2 - b)/(2\pi)$ and, therefore, period- k orbits are defined by

$$x_t^2 + y_t^2 = \frac{\pi}{2a} \left(1 - \frac{4p}{k} - \frac{2b}{\pi} \right). \quad (9)$$

Since the left-hand side of Eq. (9) is non-negative, for $a > 0$ period- k orbits exist only when $b < \beta_{k,p} \equiv (\pi/2) - 2\pi p/k$, while for $a < 0$ one must have $b > \beta_{k,p}$. When $b \rightarrow \beta_{k,p}$ all period- k orbits converge to the origin, i.e., to the fixed point $r_t = 0$. The same occurs when $a \rightarrow \infty$ and, since a is a scaling of the boson density potential, one concludes, as expected, that when the density diverges all oscillation modes vanish and the oscillators 'freeze' at $r_t = 0$. Moreover, when $a \rightarrow 0$ the amplitudes of local oscillators diverge, due to the vanishing of boson density.

Next, we determine which period- k orbits are observed for each pair (a, b) , in order to characterize the entire parameter space. Since we want to determine the existence

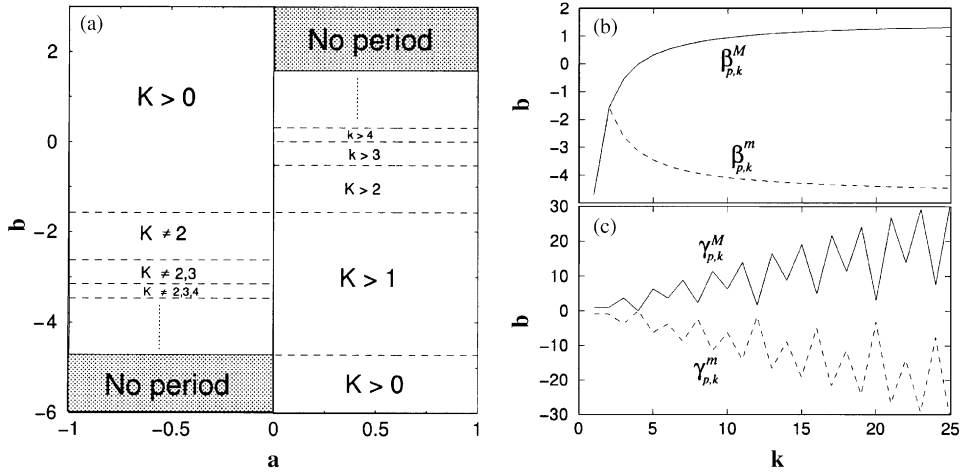


Fig. 1. Distribution of all period- k orbits in parameter space for (a) the exponential map $F_1(\Psi_t)$, Eq. (6). The regions where period- k orbits are observed have an upper boundary $\beta_{p,k}^M$ for $a > 0$ and a lower boundary $\beta_{p,k}^m$ for $a < 0$, both illustrated in (b) as functions of k , where solid line indicates the boundary for $a > 0$ and dashed line the boundary for $a < 0$. For (c) the Crank–Nicholson map $F_2(\Psi_t)$, Eq. (7), both boundaries ($\gamma_{p,k}^M$ and $\gamma_{p,k}^m$) depend quite differently on the period k (see text).

of *at least* one period- k orbit, for $a > 0$ we take the maximum of $\beta_{p,k}$ with respect to p , namely $\beta_{p,k}^M = \beta_{1,k}$, while for $a < 0$, we consider the corresponding minimum $\beta_{p,k}^m = \beta_{k-1,k}$. Fig. 1a shows an illustrative scheme of the entire parameter space, indicating the distribution of periodic orbits for the exponential map. Notice that even in the regions of ‘no period’ there is always the fixed point at the origin $(x, y) = (0, 0)$. In Fig. 1b both boundaries, $\beta_{p,k}^M$ and $\beta_{p,k}^m$, are plotted as functions of the period k , emphasizing the convergence towards the ‘no-period’ region, namely $\beta_{p,k}^M \rightarrow \pi/2$ ($a > 0$) and $\beta_{p,k}^m \rightarrow -3\pi/2$ ($a < 0$).

The distribution of periodic orbits for the exponential map is significantly changed when one considers the Crank–Nicholson discretization of Eq. (6), i.e., when one considers the Crank–Nicholson map in Eq. (7).

Written in the form of Eq. (8) the Crank–Nicholson map reads

$$\phi(r_t) = \frac{1}{2\pi} \arctan\left(\frac{1 - A_t^2}{2A_t}\right), \tag{10}$$

where $A_t = ar_t^2 + b$ and, as above, equating $\phi(r_t) = p/k$ yields

$$x_t^2 + y_t^2 = -\frac{1}{a} \left(\tan\left(\frac{p\pi}{k} \mp \frac{\pi}{4}\right) + b \right). \tag{11}$$

Using the same procedure as for the exponential map, Eq. (11) shows that when $a > 0$ period- k orbits are observed only for $b < \gamma_{p,k}^M$, where $\gamma_{p,k}^M \equiv \max_p[\tan(-p\pi/k \pm \pi/4)]$, while when $a < 0$ one finds $b > \gamma_{p,k}^m$ with $\gamma_{p,k}^m \equiv \min_p[\tan(-p\pi/k \pm \pi/4)]$. Fig. 1c shows both the maxima $\gamma_{p,k}^M$ and minima $\gamma_{p,k}^m$ as functions of period k .

Comparing Fig. 1c with 1b, one concludes that the Crank–Nicholson scheme introduces several changes in the distributions of periodic orbits. First, when $k \rightarrow \infty$ (quasi-periodicity), the boundaries of the Crank–Nicholson map diverge ($\gamma_{p,k}^M, \gamma_{p,k}^m \rightarrow \infty$), while for the exponential map one finds finite limits, namely $\beta_{p,k}^M \rightarrow \pi/2$ and $\beta_{p,k}^m \rightarrow -3\pi/2$. Second, while for the exponential map the boundaries vary monotonically with k , for the Crank–Nicholson map one observes an alternating increase and decrease of the boundary. Finally, notice the divergence of the lower boundary for period-4 orbits of the Crank–Nicholson map, meaning that, differently from the exponential map, for $a < 0$ one observes period-4 orbits for *any* value of parameter b .

4. Discussion and conclusions

In this paper, we derived a CML model characterized by complex amplitudes and by norm preserving local dynamics. The model was obtained with suitable changes in the usual Crank–Nicholson scheme of the nonlinear Schrödinger equation to guarantee that at each time-step local states depend on local and neighboring states of the previous time-step alone. Identifying each site in the lattice as a quantum system by itself, we also imposed local norm preservation and compared the distribution of periodic orbits for two possible local dynamics, one ruled by the exponential map and another by its Crank–Nicholson discretization. It should be very interesting to investigate the possible behaviors of global states (patterns) emerging in a lattice of inhomogeneous (nonidentical) maps, for instance, one governed by Eq. (5) with b_j varying randomly along the lattice.

In conclusion, this paper provides an important bridge showing that the familiar Crank–Nicholson discretization scheme may be in fact quite naturally identified with a coupled map lattice having norm-preserving complex local amplitudes. This fact opens a number of new possibilities for applications that we hope to report soon.

Acknowledgements

PGL thanks *Fundação para a Ciência e a Tecnologia*, Portugal, for a postdoctoral fellowship. JACG is a CNPq Research Fellow, Brazil.

References

- [1] I.S. Aranson, L. Kramer, Rev. Mod. Phys. 74 (2002) 99.
- [2] M.C. Cross, P.C. Hohenberg, Rev. Mod. Phys. 65 (1993) 851.
- [3] D. Henning, G.P. Tsironis, Phys. Rep. 307 (1999) 333.
- [4] R. Baer, Phys. Rev. A 62 (2000) 063810.
- [5] C. Lobo, A. Sinatra, Y. Castin, Phys. Rev. Lett. 92 (2004) 020403.
- [6] J.D. Carter, H. Segur, Phys. Rev. E 68 (2003) 045601(R).
- [7] P.G. Kevrekedis, K.Ø. Rasmussen, A.R. Bishop, Int. J. Mod. Phys. B 15 (2001) 2833–2900.
- [8] B. Rumpf, Phys. Rev. E 69 (2004) 016618.
- [9] D.E. Pelinovsky, P.G. Kevrekidis, D.J. Frantzeskakis, Phys. Rev. Lett. 91 (2003) 240201.

- [10] M. Soljai, K. Steiglitz, S.M. Sears, M. Segev, M.H. Jakubowski, R. Squier, *Phys. Rev. Lett.* 90 (2003) 254102.
- [11] T.K. Kopeć, J.V. José, *Phys. Rev. Lett.* 84 (2000) 749–752.
- [12] P.J. Martínez, L.M. Flórida, F. Falo, J.J. Mazo, *Europhys. Lett.* 45 (1999) 444–449.
- [13] K. Kaneko, I. Tsuda, *Chaos and Beyond*, Springer, Berlin, 2000.
- [14] S. Jalan, R.E. Amritkar, *Phys. Rev. Lett.* 90 (2003) 014101.
- [15] G. Boffetta, D. del-Castillo-Negrete, C. López, G. Pucacco, A. Vulpiani, *Phys. Rev. E* 67 (2003) 026224.
- [16] C. Hauptmann, H. Touchette, M.C. Mackey, *Phys. Rev. E* 67 (2003) 026217.
- [17] P.G. Lind, J. Corte-Real, J.A.C. Gallas, *Phys. Rev. E* 66 (2002) 016219.
- [18] F.H. Willeboordse, *Phys. Rev. E* 65 (2002) 026202.
- [19] N.F. Rulkov, *Phys. Rev. E* 65 (2002) 041922.
- [20] O. Popovych, Yu. Maistrenko, E. Mosekilde, *Phys. Rev. E* 64 (2001) 026205.
- [21] A.K. Pattanayak, B. Sundaram, B.D. Greenbaum, *Phys. Rev. Lett.* 90 (2003) 014103.
- [22] W.H. Press, S.A. Teukolsky, W.T. Vetterling, B.P. Flannery, *Numerical Recipes in Fortran*, Cambridge University Press, USA, 1992.